

Senolytic therapy to modulate the progression of Alzheimer's Disease (SToMP-AD) – Outcomes from the first clinical trial of senolytic therapy for Alzheimer's disease

Miranda Orr (✉ morr@wakehealth.edu)

Wake Forest School of Medicine <https://orcid.org/0000-0002-0418-2724>

Mitzi Gonzales

University of Texas Health Science Center

Valentina Garbarino

University of Texas Health Science Center

Tiffany Kautz

University of Texas Health Science Center

Juan Palavicini

University of Texas Health Science Center <https://orcid.org/0000-0001-9667-8438>

Marisa Lopez-Cruzan

University of Texas Health Science Center <https://orcid.org/0000-0003-0285-1012>

Shiva Kazempour Dehkordi

University of Texas Health Science Center <https://orcid.org/0000-0003-0349-4360>

Julia Mathews

University of Texas Health Science Center

Habil Zare

University of Texas Health Science Center

Peng Xu

Department of Genetics and Genomic Sciences, Icahn School of Medicine at Mount Sinai

<https://orcid.org/0000-0001-8007-9879>

Bin Zhang

Icahn School of Medicine at Mount Sinai

Crystal Franklin

University of Texas Health Science Center

Mohamad Habes

German Center for Neurodegenerative Diseases (DZNE)

Suzanne Craft

Wake Forest University Health Sciences

Ronald Petersen

Mayo Clinic Minnesota <https://orcid.org/0000-0002-8178-6601>

Tamara Tchkonja

Mayo Clinic <https://orcid.org/0000-0003-4623-7145>

James Kirkland

Mayo Clinic <https://orcid.org/0000-0003-1676-4905>

Arash Salardini

University of Texas Health Science Center

Sudha Seshadri

University of Texas Health Science Center

Nicolas Musi

University of California

Article

Keywords:

Posted Date: April 24th, 2023

DOI: <https://doi.org/10.21203/rs.3.rs-2809973/v1>

License:  This work is licensed under a Creative Commons Attribution 4.0 International License.

[Read Full License](#)

Additional Declarations: **Yes** there is potential Competing Interest. Dr. Gonzales reports personal stock in Abbvie. Dr. Petersen reports personal fees from Roche, personal fees from Merck, personal fees from Biogen, personal fees from Eisai, personal fees from Genentech, outside the submitted work. Drs. Kirkland and Tchkonja have a patent Killing Senescent Cells and Treating Senescence-Associated Conditions Using a SRC Inhibitor and a Flavonoid with royalties paid to Unity Biotechnologies, and a patent Treating Cognitive Decline and Other Neurodegenerative Conditions by Selectively Removing Senescent Cells from Neurological Tissue with royalties paid to Unity Biotechnologies. Dr. Craft reports other from vTv Therapeutics, other from Cylcerion, other from T3D Therapeutics, from Cognito Therapeutics, outside the submitted work. Dr. Orr has a patent Biosignature and therapeutic approach for neuronal senescence pending.

1 **Senolytic therapy to modulate the progression of Alzheimer's Disease (SToMP-AD) –**
2 **Outcomes from the first clinical trial of senolytic therapy for Alzheimer's disease**

3 Mitzi M. Gonzales, PhD^{1,2}, Valentina R. Garbarino, PhD^{1,3}, Tiffany Kautz, PhD^{1,3}, Juan Pablo
4 Palavicini, PhD³, Marisa Lopez-Cruzan, PhD⁴, Shiva Kazempour Dehkordi, MS^{1,5}, Julia
5 Mathews, BS¹, Habil Zare, PhD^{1,5}, Peng Xu, PhD^{6,7}, Bin Zhang, PhD^{6,7}, Crystal Franklin⁸,
6 Mohamad Habes, PhD^{1,9}, Suzanne Craft, PhD¹⁰, Ronald C. Petersen, MD¹¹, Tamara Tchkonina,
7 PhD¹², James Kirkland, MD¹³, Arash Salardini, MD^{1,2}, Sudha Seshadri, MD^{1,2,14}, Nicolas Musi,
8 MD^{3,15}, Miranda E. Orr, PhD¹⁰

9 ¹Glenn Biggs Institute for Alzheimer's & Neurodegenerative Diseases, University of Texas Health
10 Science Center at San Antonio, San Antonio, TX, USA

11 ²Department of Neurology, University of Texas Health Science Center at San Antonio, San
12 Antonio, TX, USA

13 ³Department of Medicine, University of Texas Health Science Center at San Antonio, San Antonio,
14 TX, USA

15 ⁴Department of Psychiatry, University of Texas Health Science Center at San Antonio, San
16 Antonio, TX, USA

17 ⁵Department of Cell Systems and Anatomy, University of Texas Health Science Center at San
18 Antonio, San Antonio, TX, USA

19 ⁶Department of Genetics and Genomic Sciences, Icahn School of Medicine at Mount Sinai, New
20 York, NY, USA

21 ⁷Mount Sinai Center for Transformative Disease Modeling, Icahn School of Medicine at Mount
22 Sinai, New York, NY, USA

23 ⁸Research Imaging Institute, University of Texas Health Science Center at San Antonio, San
24 Antonio, TX, USA

25

26 ⁹Department of Radiology, University of Texas Health Science Center at San Antonio, San
27 Antonio, TX, USA

28 ¹⁰Department of Internal Medicine Section on Gerontology and Geriatric Medicine, Wake Forest
29 School of Medicine, Winston-Salem, NC, USA

30 ¹¹Department of Neurology, Mayo Clinic, Rochester, MN, USA

31 ¹²Department of Physiology and Biomedical Engineering, Mayo Clinic, Rochester, MN, USA

32 ¹³Department of Internal Medicine, Mayo Clinic, Rochester, MN, USA

33 ¹⁴Department of Neurology, Boston University School of Medicine, Boston, MA, USA

34 ¹⁵Department of Geriatric Medicine, Cedars-Sinai Medical Center, Los Angeles, CA, USA

35

36

37

38 **Abstract**

39 Cellular senescence has been identified as a pathological mechanism linked to tau and amyloid
40 beta (A β) accumulation in mouse models of Alzheimer's disease (AD). Clearance of senescent
41 cells using the senolytic compounds dasatinib (D) and quercetin (Q) reduced neuropathological
42 burden and improved clinically relevant outcomes in the mice. Herein, we conducted a vanguard
43 open-label clinical trial of senolytic therapy for AD with the primary aim of evaluating central
44 nervous system (CNS) penetrance, as well as exploratory data collection relevant to safety,
45 feasibility, and efficacy. Participants with early-stage symptomatic AD were enrolled in an open-
46 label, 12-week pilot study of intermittent orally-delivered D+Q. CNS penetrance was assessed
47 by evaluating drug levels in cerebrospinal fluid (CSF) using high performance liquid
48 chromatography with tandem mass spectrometry. Safety was continuously monitored with
49 adverse event reporting, vitals, and laboratory work. Cognition, neuroimaging, and plasma and
50 CSF biomarkers were assessed at baseline and post-treatment. Five participants (mean age:
51 76 \pm 5 years; 40% female) completed the trial. The treatment increased D and Q levels in the
52 blood of all participants ranging from 12.7 to 73.5 ng/ml for D and 3.29-26.30 ng/ml for Q. D
53 levels were detected in the CSF of four participants ranging from 0.281 to 0.536 ng/ml
54 ($t(4)=3.123$, $p=0.035$); Q was not detected. Treatment was well-tolerated with no early
55 discontinuation and six mild to moderate adverse events occurring across the study. Cognitive
56 and neuroimaging endpoints did not significantly differ from baseline to post-treatment. CNS
57 levels of IL-6 and GFAP increased from baseline to post-treatment ($t(4)=3.913$, $p=0.008$ and
58 $t(4)=3.354$, $p=0.028$, respectively) concomitant with decreased levels of several cytokines and
59 chemokines associated with senescence, and a trend toward higher levels of A β 42 ($t(4)=-2.338$,
60 $p=0.079$). Collectively the data indicate the CNS penetrance of D and provide preliminary
61 support for the safety, tolerability, and feasibility of the intervention and suggest that astrocytes
62 and A β may be particularly responsive to the treatment. While early results are promising, fully

63 powered, placebo-controlled studies are needed to evaluate the potential of AD modification
64 with the novel approach of targeting cellular senescence.

65

66 **Introduction**

67 Alzheimer's disease (AD) is the most prevalent cause of dementia, a devastating
68 condition that affects over 35 million individuals worldwide¹. Historically, drug development for
69 the indication of AD has been among the slowest, most expensive, and least successful with a
70 failure rate of over 99%². Fortunately, recent years have seen the development of disease
71 modifying drugs capable of removing abnormal aggregations of amyloid beta (A β) from the
72 brain³. Despite these successes, the anti-amyloid drugs have only yielded modest clinical
73 results, spurring consideration of new drug targets and combination treatments^{3,4}.

74 The majority of individuals with AD present with multiple etiological contributors to
75 dementia⁵, suggesting that therapeutic targets beyond A β and tau deposition may have a role in
76 treatment. Towards this end, our preclinical research has highlighted cellular senescence as a
77 mechanism that may underlie pathological tau accumulation^{6,7}. Cellular senescence is a
78 complex stress response triggered by various stimuli, including macromolecular damage (such
79 as DNA damage), proteotoxic stress, oncogene activation, reactive metabolites, mitochondrial
80 dysfunction, and infections, among others⁸. The stress response leads to a change in cell fate
81 whereby senescent cells enter a near-permanent cell cycle arrest mediated through tumor
82 suppressive pathways⁹. Senescent cells also acquire a senescence-associated secretory
83 phenotype (SASP)^{10,11}. The SASP is comprised of cytokines, chemokines, growth factors, and
84 extracellular matrix re-modeling components, which can spread in a paracrine manner and
85 propagate the senescent phenotype to neighboring cells^{8,12}. In the context of aging and
86 neurodegenerative disease, senescent cell accumulation has been identified in multiple cell
87 types within the central nervous system, including neurons^{6,7,13,14}, astrocytes^{15,16}, microglia^{17,18},
88 oligodendrocyte precursor cells¹⁹, and endothelial cells²⁰.

89 Experimental evidence to support the role of cellular senescence in AD neuropathology
90 has been provided by preclinical trials employing senolytics. Senolytics are pharmacological

91 agents which selectively ablate senescent cells and were first identified through interrogation of
92 the senescent cell anti-apoptotic pathways (SCAPs)²¹. At present, dasatinib (D), a tyrosine-
93 kinase inhibitor that is FDA-approved for chronic myeloid leukemia (CML) and acute
94 lymphoblastic leukemia (ALL)²², and quercetin (Q), a natural plant-based flavonoid with anti-
95 inflammatory, antioxidant, and antineoplastic properties²³, are the best characterized
96 senolytics⁸. When combined, D+Q has been shown to selectively clear senescent cells in
97 culture in both humans and animal models^{8,24,25}. In preclinical trials of murine models, D+Q has
98 ameliorated multiple chronic age-related conditions; we previously reported the first evidence to
99 support the potential therapeutic efficacy of D+Q for neurodegenerative disease. Within four tau
100 transgenic mouse models, we found that biweekly administration of D+Q relative to placebo
101 resulted in a 35% reduction in cortical NFT accumulation, which correlated with reduced cortical
102 brain atrophy and restored aberrant cerebral blood flow⁶. Other research teams confirmed the
103 association between tau and senescence¹⁸ and the effective clearance of senescent cells using
104 D+Q in an A β producing mouse model¹⁹.

105 Given the compelling evidence provided by preclinical research^{6,19}, coupled with the
106 encouraging safety profiles reported in human studies of D+Q for other disease indications^{26,27},
107 we conducted the first clinical trial of senolytic therapy for AD. The aim of the study was to
108 evaluate penetration of D and Q in the central nervous system by performing mass
109 spectrometry on cerebral spinal fluid (CSF) collected prior to treatment and within 80 to 150
110 minutes of the final study drug dose. We further aimed to collect data on secondary outcomes
111 including safety and feasibility, target engagement of the senolytic compounds, AD CSF and
112 plasma biomarkers, and cognition, neuroimaging, and functional status. We enrolled five
113 participants with early-stage symptomatic AD in an open-label 12-week intervention of
114 intermittent senolytic therapy and provide the first report of the trial outcomes.

115 **Methods**

116 The study is an open-label single-site pilot study of 12-week intermittent senolytic therapy in
117 older adults with early-stage AD with the primary aim of evaluating the central nervous system
118 penetrance of D and Q (NCT04063124)²⁸. Secondary trial aims were to 1) evaluate target
119 engagement of D+Q by examining changes markers associated with cellular senescence and
120 the SASP; 2) assess the safety and tolerability of the intervention; 3) examine pre- to post-
121 treatment changes in cognition and functional status; and 4) assess changes in neuroimaging
122 and biofluid markers of AD and related dementias (ADRD). The study was conducted in
123 adherence with the Guideline for Good Clinical Practice and the protocol was approved by the
124 local institutional review board. All participants provided written informed consent with
125 appropriate legal representation for individuals lacking capacity to consent.

126 Participants: Eligibility for the study included adults aged 65 years and over with a diagnosis of
127 AD based on the criteria for the National Institute on Aging-Alzheimer's Association²⁹ and a
128 Global Clinical Dementia Rating (CDR) Scale score of 1³⁰. Anticholinesterase inhibitors and/or
129 memantine use were allowed following a minimum of a three-month stabilization period. Full
130 eligibility criteria were applied as described in Gonzales et al²⁸.

131 Study Design: As previously described²⁸, the study protocol included completion of 11 study
132 visits over a period of 20 to 24 weeks (Figure 1). Following obtainment of written informed
133 consent, study candidates completed an in-person screening visit consisting of a blood draw,
134 vital signs, anthropomorphic measurements, physical and neurological examination, medical
135 history and concomitant medication reviews, cognitive screening assessments (CDR³⁰ and
136 Montreal Cognitive Assessment (MoCA)³¹), and electrocardiogram (ECG). Following
137 confirmation of study eligibility, participants completed two baseline assessment visits consisting
138 of a fasting blood draw and lumbar puncture (Baseline Visit 1) and assessments of cognition,
139 functional status, and an optional brain MRI (Baseline Visit 2). In response to the onset of the
140 COVID-19 pandemic, the protocol was modified to include confirmation of a negative real-time
141 reverse transcriptase–polymerase chain reaction (rRT-PCR) test within 72 hours of the first

142 study drug administration, and COVID-19 symptom and exposure screenings were conducted
143 across the study. The first study drug administration visit occurred within 3 to 10 days of the
144 second baseline visit. Study drugs, 100mg of D (one 100mg capsule, Sprycel, Bristol Meyers
145 Squibb) and 1000mg of Q (four 250 mg capsules, Thorne Research) were administered
146 consecutively for two days followed by a 13- to 15-day study drug holiday across a total of six
147 cycles (IND #143945). On the first day of each cycle, participants reported to the study site for
148 safety assessments and drug dispensing. Within 80 to 150 minutes of the administration of final
149 study drug dose, participants underwent a fasting blood draw and lumbar puncture. The
150 assessment procedures administered at Baseline Visit 2 were repeated within 3-10 days of the
151 final study drug dose. D+Q were administered under IND # 143945-0006 (to N.M).

152 Safety and Adherence: Vital signs, concomitant medications, and adverse events were
153 reviewed at each study visit. Safety labs, including complete blood count (CBC) with differentials
154 and comprehensive metabolic panel (CMP) with liver and lipid panels, were conducted at Visits
155 1, 4, 5, 6, 8, and 9. Prothrombin time/partial thromboplastin time/international normalized ratio
156 (PT/PTT/INR) was assessed at Visits 1 and 8 and hemoglobin A1c (HbA1c) was evaluated at
157 Visits 1 and 9. Electrocardiogram was conducted at Visits 1, 4, 6, 8, and 11. The study was
158 monitored by an independent data and safety monitoring board, who reviewed the safety data
159 on an annual basis. Adherence was assessed by the total number of doses completed, counted
160 by administrations in clinic, home diary records, and pill bottle review.

161 Cognitive and Functional Outcomes: The pre-specified cognitive outcomes of interest were pre-
162 to post-treatment changes on the MoCA³¹ and CDR Sum of Boxes (SOB)³⁰. Additional cognitive
163 assessments included the Weschler Memory Scale Fourth Edition (WMS-IV) Logical Memory³²,
164 Benson Figure³³, Trail Making Test Parts A&B³³, Number Span Test³³, Category Fluency³⁴,
165 Phonemic Fluency³⁴, Boston Naming Test³⁵, and the Hopkins Verbal Learning Test Revised
166 (HVLT-R)³⁶. Neuropsychiatric symptoms were assessed using the self-reported Geriatric
167 Depression Scale 15-Item (GDS-15) and informant-reported Neuropsychiatric Inventory (NPI)³³.

168 Functional status was evaluated using the informant-reported Lawton IADL form³⁷ and as part of
169 the CDR.

170 Brain MRI: Brain MRI was conducted at the UTHSCSA Research Imaging Institute on a 3-Tesla
171 Siemens Trio scanner. The imaging protocol consisted of a localizer scan, high-resolution 3-
172 dimensional T1-weighted structural series scan, a T2-weighted fluid attention inversion recovery
173 (FLAIR) scan, a diffusion-weighted scan, and a gradient echo scan. Pre- and post-treatment
174 structural scans were spatially coregistered using rigid-body registration, followed by nonlinear
175 registration and multi-atlas based neuroanatomic parcellation,³⁸⁻⁴⁰ to quantify total brain and
176 hippocampal volume and grey and white matter density normalized to intracerebroventricular
177 volume (ICV) from four of the five study participants.

178 Blood Draws and Lumbar Punctures: Blood plasma and CSF samples for research purposes
179 were collected according to established procedures⁴¹. Briefly, blood was collected under fasting
180 conditions via venipuncture in a plasma EDTA vacutainer tube (BD, Franklin Lakes, NJ),
181 inverted 5-10 times, and centrifuged at 2000 x *g* for 10 minutes at room temperature. Plasma
182 was aliquoted and stored at -80°C within 2 hours of collection. CSF was also collected under
183 fasting conditions using a 24-gauge atraumatic Sprotte spinal needle under gravity flow
184 (Teleflex, Morrisville, NC). CSF was collected into a sterile polypropylene tube (Rose Scientific,
185 Alberta, CA), which was centrifuged at 2000 x *g* for 10 minutes at room temperature. CSF was
186 aliquoted and stored at -80°C within 2 hours of collection.

187 Assays

188 Drug Concentrations: Pre- and post-treatment D and Q concentrations in blood and CSF
189 were quantified via High Performance Liquid Chromatography (HPLC) with Tandem Mass
190 Spectrometry detection (MS/MS) method (HPLC/MS/MS) at the UTHSCSA Biological
191 Psychiatry Analytical Lab. Analytical solutions were prepared with Milli-Q Plus water (Millipore
192 Sigma, EMD Millipore, Billerica, MA). D and Q analytical standards were obtained from Sigma
193 (Sigma-Aldrich Corp., St. Louis, MO) and their metabolites (dasatinib n-oxide and 4-o-methyl

194 quercetin) and internal standards (IS) from Cayman (Cayman Chemical, Ann Arbor, MI). All
195 other chemicals were HPLC analytical grade and purchased from Fisher Scientific (Thermo
196 Fisher Scientific, Waltham, MA). Tandem mass spectrometry was performed using a Shimadzu
197 8045 Triple Quadrupole mass spectrometer (Shimadzu Scientific Instruments, Inc., Houston,
198 TX). The lower limit of detection (LOD) was estimated to be 0.3 ng/ml for D, Q, and their
199 metabolites in plasma and CSF, except for D in CSF, which was estimated to be 0.025 ng.ml.
200 The lower limit of quantitation (LOQ) for D, Q and their metabolites was estimated to be 1.0
201 ng.ml, except for D in CSF which was estimated to be 0.2 ng/ml.

202 Markers of Cellular Senescence and SASP: The Mesoscale Discovery U-Plex Biomarker
203 Group 1 (hu) 71-plex panel (MesoScale Discovery, Natickm MA) was used to measure IL-6, a
204 prespecified secondary outcome, and additional cytokines and chemokines in CSF and plasma.
205 Samples were diluted and measured in duplicate, as per the manufacturer's protocol. A MESO
206 QuickPlex SQ 120MM instrument was used to measure the concentration of each marker.

207 ADRD Biomarkers: A Simoa HD-X analyzer (Quanterix, Lexington, MA) was used to
208 measure phosphorylated tau (p-Tau) 181 (SIMOA pTau-181 Advantage V2 kit, Quanterix,
209 Lexington, MA), A β 40, A β 42, glial fibrillary acidic protein (GFAP), and neurofilament light (NFL)
210 (SIMOA Neuro 4-Plex E Advantage kit, Quanterix, Lexington, MA) concentrations in plasma and
211 CSF. The SIMOA pTau-231 Advantage kit (Quanterix, Lexington, MA) was used to measure
212 pTau 231 concentration in CSF. Prior to loading the samples onto the Simoa analyzer, plasma
213 and CSF samples were clarified by centrifugation at 14,000 x g for 10 minutes. All samples were
214 run in duplicate. In addition, a Fujirebio G1200 (Malvern, PA) was used to measure total tau
215 (lumipulse G total tau, Malvern, PA), pTau-181 (lumipulse G pTau-181, Malvern, PA) A β 40
216 (lumipulse G B-Amyloid 1-40, Malvern, PA), and A β 42 (lumipulse G B-Amyloid 1-42, Malvern,
217 PA) as per the manufacturer's protocol.

218 **Statistical Analysis:**

219 Descriptive analyses were performed on baseline demographic and broader sample
220 characteristics. Baseline to post-treatment changes in safety labs, vitals and body mass index
221 (BMI), cognitive and functional assessment, neuroimaging outcomes, and biofluid markers were
222 assessed using paired samples t-tests. All analyses were performed using SPSS version 28.0.
223 Statistical tests were 2-sided and statistical significance was set at $p < 0.05$. Given the
224 exploratory nature of the pilot study, p-values were not corrected for multiple comparisons
225 unless otherwise noted in the text.

226 **Results:**

227 Participants: A total of 21 participants were screened over the phone, eight of whom did not
228 meet the eligibility criteria (Figure 2). Thirteen participants completed the in-person screening
229 visit and of those, seven were screen failures and one withdrew. Five participants (aged 70-82
230 years; median 76; 40% female; 80% Non-Hispanic White; 20% Hispanic) enrolled in the
231 intervention. Regarding highest level of educational attainment, two participants (40%) had high
232 school diplomas, one (20%) had some college, and two participants (40%) had college degrees
233 or higher.

234 Safety and Adherence: A total of six adverse events (AEs) occurred during the course of the
235 study, of which three (two mild: diarrhea and emesis, urinary tract infection, one moderate:
236 hypoglycemia) occurred following the start of the intervention. The two mild AEs were deemed
237 unlikely related to the study and the one moderate AE, hypoglycemia, was deemed possibly
238 related to the intervention. Prior to the start of the intervention, there was one moderate severity
239 AE (fall resulting in hematoma) and two mild AEs (hematuria, diarrhea). All AEs fully resolved
240 within one to 16 days.

241 There were no significant changes in BMI (pre-treatment: 23.0 ± 4.3 mg/k²; post-
242 treatment: 22.7 ± 4.2 mg/kg², $t(4) = -1.12$, $p = 0.32$), systolic blood pressure (pre-treatment:
243 114.4 ± 11.8 mmHg; post-treatment: 120.4 ± 16.7 mmHg, $t(4) = 0.56$, $p = 0.61$) or diastolic blood
244 pressure (pre-treatment: 63.8 ± 14.3 mmHg; post-treatment: 67.4 ± 9.2 mmHg, $t(4) = 0.96$, $p = 0.39$).

245 There was a statistically significant, but not clinically significant, increase in total
246 cholesterol from pre- to post-treatment (pre-treatment: 169.2 \pm 35.5 mg/dl; post-treatment:
247 179.4 \pm 40.0 mg/dl, $t(4)=2.904$, $p=0.044$). No other significant changes in safety lab parameters
248 were observed (Supplementary Table 1).

249 All five participants who enrolled in the intervention completed the trial with a 100%
250 study drug adherence rate.

251 Study Drug Concentrations: As expected, D was not present in plasma or CSF prior to
252 treatment (Figure 3A-B). After the intervention, D was detected in plasma in all five participants,
253 ranging from 12.7 to 73.5 ng/ml. In CSF, post-treatment D levels were slightly above the LOQ
254 (0.2 ng/ml) in four out of five participants, ranging from 0.281 to 0.536 ng/ml, and the fifth had no
255 detectable levels. In the four participants with detection of D in CSF, the CSF to plasma ratio of
256 D concentrations ranged from 0.004 to 0.008. D metabolites were undetected in both plasma
257 and CSF with the exception of one post-treatment plasma specimen, 1.94 ng/ml (LOQ 1.0
258 ng/ml; metabolite data not shown).

259 Q is found in many fruits and vegetables^{42,43}. In plasma at baseline, three participants
260 had no detectable Q levels and the other two had concentrations of 1.09 and 1.73 ng/ml (LOQ
261 1.0 ng/ml). However, the two participants that had Q levels just above the LOQ at baseline had
262 Q concentrations of 26.3 and 13.3 ng/ml post-treatment. Following treatment, Q was detected in
263 plasma across participants, ranging from 3.29-26.30 ng/ml (Figure 3C). Within CSF, Q was not
264 detected either before or after treatment across participants. Q metabolites were detected only
265 in two post-treatment plasma specimens, 2.92 and 3.80 ng/ml (LOQ 1.0 ng/ml) and one post-
266 treatment CSF sample, 1.23 ng/ml (LOQ 1.0 ng/ml; metabolite data not shown). Within CSF, Q
267 was not detected either before or after treatment across participants.

268 Cognitive and functional outcomes: Baseline to post-treatment changes in the pre-specified
269 cognitive outcomes, MoCA and CDR SOB, were not significant (Table 1). There was a
270 statistically significant decrease on HVLT-R Immediate Recall. All other cognitive tests, as well

271 as questionnaires assessing neuropsychiatric symptoms and functional status, did not
272 demonstrate any significant changes.

273 Neuroimaging: Paired t-tests of pre- versus post-treatment MRIs revealed no significant
274 differences in total brain volume, gray matter or white matter density, or right or left hippocampal
275 volume, indicative of stable brain morphology over the three-month assessment period (Table
276 2).

277 Markers of Cellular Senescence and SASP: Applying the unadjusted $p < 0.05$ cut-off, plasma
278 levels of IL-17E, IL-21, IL-23, IL-17A/F, IL-17D, IL-10, VEGF, IL-31, MCP-2, MIP-1 β and MIP-1 α
279 decreased from pre- to post-treatment, whereas YKL-40 levels increased. In CSF, TARC, IL-
280 17A, I-TAC, Eotaxin-2, Eotaxin, and MIP-1 α levels decreased, and IL-6 levels increased from
281 pre- to post-treatment (Table 3

282 ADRD Biomarkers: Using the SIMOA assays, there were no pre- to post-treatment changes in
283 plasma or CSF protein levels with the exception of a significant increase of GFAP levels in CSF
284 (Figure 4A-K). For the Lumipulse assays, no significant treatment changes were observed in
285 CSF; however, there was a trend ($p = 0.0795$) towards higher A β 42 levels post-treatment (Figure
286 5A-F).

287 **Discussion**

288 Cellular senescence has been associated with neurodegenerative disease in human
289 pathology studies and preclinical models^{6,7,18,19}. Herein, we present the results of the first-in-
290 human trial of senolytic therapy for AD²⁸. The primary aim of our open-label pilot study was to
291 evaluate the CNS penetrance of first-generation senolytics, D and Q. Our results confirmed the
292 presence of D in CSF following treatment. In addition, the intervention was well-tolerated with no
293 premature discontinuation and only three AEs occurring following treatment initiation. Our study
294 was not designed or powered to detect efficacy. However, our preliminary data suggests the
295 potential of baseline to post-treatment changes in markers of cellular senescence and ADRD,

296 which will require further exploration and validation in randomized placebo-controlled trials that
297 are presently underway (NCT04685590).

298 A primary challenge to conducting trials for AD and other neurological diseases is the
299 determination of the appropriate drug dosing as assessing pharmacokinetics in the CNS is
300 highly invasive. In our study, we selected the combination of D and Q as they are among the
301 best characterized senolytic agents, target multiple SCAP pathways, and are repurposed^{8,25},
302 expediting clinical testing. The doses and intermittent scheduling regimen were selected based
303 on prior research demonstrating safety and early indications of efficacy for other disease
304 indications^{8,26}. The intermittent dosing regimen was implemented because senescent cells
305 across organ systems, including the brain, typically accumulate over a period of weeks,
306 suggesting that drugs do not continually need to be present to be effective^{6,21}. Intermittent
307 dosing further reduces potential toxicity. Our study design of in-clinic administrations on the first
308 day of each drug cycle enabled us to carefully monitor participant safety and was likely
309 supportive of our 100% study drug adherence rate. In plasma, D has been shown to reach peak
310 concentrations within two hours of administration⁴⁴; however, the absorption in the CNS is less
311 well established. Following oral ingestion of D in mice, a prior study reported D in brain
312 homogenates using HPLC/MS at concentrations that were 12- to 31-fold lower than in plasma⁴⁴.
313 In humans, D has demonstrated efficacy for treating ALL and CML with CNS involvement and
314 responses can be maintained for months to years⁴⁴, suggesting a robust CNS treatment effect.
315 However, HPLC/MS studies conducted in CSF taken from D-treated individuals with CML or
316 ALL have reported low CSF concentrations and high variability across individuals^{44,45}. Gong et
317 al. examined plasma and CSF concentrations of D among individuals with ALL approximately
318 two hours after a single dose of 100 mg of D⁴⁵. Detectable D levels in CSF were only observed
319 in 16% of participants (4/25 individuals) with ranges between 0.23 to 0.68 ng/ml. In our study,
320 we observed a similar range of D concentrations in CSF. However, the detectable levels were
321 more readily observed in our population, occurring in 80% (4/5 individuals) of participants. More

322 consistent CSF concentrations may have been observed in our study of individuals with AD due
323 to the disease's impact on blood brain barrier integrity⁴⁶. Future pharmacokinetic studies will be
324 helpful for informing on the optimal dosing for desired CNS effects. However, our study
325 demonstrated that D penetrated the CNS and prior research in oncology has shown that the
326 medication can demonstrate CNS efficacy at low or even subnanomolar concentrations^{44,47}.

327 In our study, Q was consistently detected in plasma across participants. However, unlike
328 D, Q was not detectable in CSF within our sample. In animal model research, oral
329 administration of Q has been shown to reduce oxidative stress in the brain^{48,49}, suggesting a
330 therapeutic effect in the CNS. In a preclinical study of mice that ingested 21.3 grams of Q per
331 day, Q was detectable in brain homogenates assessed using HPLC-tandem mass
332 spectrometry, plateauing after one-week of administration⁴⁹. In culture, Q has been shown to
333 permeate primary brain microvessel endothelial cells and primary astroglia cells⁵⁰, suggesting
334 blood brain barrier penetrance. However, confirmatory studies in humans are lacking. Q is
335 rapidly metabolized in the human intestinal mucosa and liver and it has low bioavailability⁵¹,
336 which may explain why it was not detectable in CSF within our study. There are ongoing efforts
337 to improve the CNS permeability with the use of nanoparticles and/or chemical modification⁴⁹.
338 Further pharmacokinetic studies of Q in humans are warranted.

339 As the first-in-human clinical trial of senolytic therapy for AD, our study also provides
340 important preliminary data on safety, tolerability, and feasibility. Throughout the study, a total of
341 six AEs occurred, of which three emerged after treatment initiation. Two of these AEs were mild
342 and highly common in the study population. Hypoglycemia was observed in one participant. D
343 has been associated with changes in glucose regulation with reports of both hyper- and
344 hypoglycemia emerging^{52,53}. It has been hypothesized that the responses may differ depending
345 on age, genetics, and comorbidity burden⁵³. Without larger sample sizes and a placebo group,
346 we are unable to determine if hypoglycemia occurred more frequently in the active treatment
347 arm. Regular assessments of glucose levels in future trials may be helpful for further

348 clarification. Clinical safety labs were generally stable from baseline to post-treatment. Only one
349 statistically significant change emerged, which was an increase in total cholesterol levels.
350 However, cholesterol levels remained in the normative range. A prior retrospective study
351 conducted in adults with CML and normal baseline glucose-lipid levels suggested that D may
352 cause mild increases in glucose, triglyceride and LDL-cholesterol levels⁵³. In contrast to the
353 typical treatment of CML, the intermittent dosing approach used in this trial may have helped to
354 attenuate metabolic changes.

355 Our study was not powered to examine target engagement, but instead designed to
356 collect exploratory data on baseline to post-treatment changes in markers of cellular
357 senescence and SASP both in CSF and blood. Change in IL-6 was a prespecified secondary
358 outcome. The analyses revealed a statistically significant elevation of IL-6 in CSF after
359 treatment. Plasma levels modestly increased, but did not reach statistical significance. The
360 treatment-induced changes in IL-6 may reflect senescent cell apoptosis whereby IL-6 was
361 directly released from senescent cells upon their lysis; alternatively, apoptosis may have
362 initiated an immune response to clear the cellular debris. Recognizing that IL-6 is a pleiotropic
363 cytokine, we simultaneously performed a broader evaluation of cytokines and chemokines to
364 better infer the treatment effect. CSF analyses indicated baseline to post-treatment decreases in
365 adaptive immunity markers, TARC, IL-17A, I-TAC, Eotaxin and Eotaxin-2; and chemokine, MIP-
366 1 α . A similar pattern was observed in plasma whereby treatment was associated with a
367 decrease in adaptive immunity markers IL-23, IL-21, IL-17, IL-31, and VEGF⁵⁴; and chemokines,
368 MIP-1 α and MIP-1 β . Given that senescent cells secrete these molecules as SASP factors, the
369 observed reduction support a decrease in senescent cell burden post-treatment. While the
370 majority of markers displayed reductions from pre- to post-treatment, there was variability. It is
371 important to highlight that none of the markers would have withstood multiple comparisons

372 correction, and the preliminary findings require further replication in studies designed to assess
373 this endpoint.

374 Consistent with AD trials, our study also acquired cognitive and neuroimaging measures.
375 Baseline to post-treatment changes were not observed for our pre-specified cognitive endpoints,
376 the MoCA and CDR SOB. The null findings are not surprising as our trial was not designed to
377 evaluate efficacy and included a small sample size and short duration of treatment. Prior studies
378 in AD suggest that study durations of 18-months are required to observe decline in placebo
379 groups⁵⁵, providing a framework for trial lengths to assess efficacy. In our exploratory
380 assessment of the broader cognitive battery, baseline to post-treatment performances were
381 stable. There was a statistically significant decrease on a verbal learning measure (HVLTR),
382 however, without a control group, we are unable to compare the findings relative to the natural
383 neurodegenerative disease course. Regarding neuroimaging outcomes, there were not
384 significant changes in total brain volume, hippocampal volume, or gray matter or white matter
385 density from baseline to post-treatment. While our study was underpowered and of insufficient
386 duration to provide a comprehensive evaluation of neuroimaging outcomes, we consider the
387 absence of changes to indicate a favorable safety profile of senolytic treatment. The data further
388 underscore the need for randomized clinical trials designed to evaluate these metrics.

389 As a secondary outcome, our study also evaluated key ADRD biomarkers in both
390 plasma and CSF at baseline and post-treatment. There were no significant changes in plasma
391 biomarkers, which was anticipated given the small sample size and short follow-up period. In
392 CSF, we observed a significant increase in GFAP levels from baseline to post-treatment. CSF
393 GFAP levels are presumed to reflect reactive astrogliosis⁵⁶ and demonstrate elevations early in
394 the neurodegenerative disease process⁵⁷. In our study, it is unclear if increases in GFAP reflect
395 or an acute response to treatment. Coupled with the elevated CSF IL-6 data, it is tempting to
396 speculate that the concomitant increase in GFAP may reflect apoptosis of senescent astrocytes.
397 Supporting evidence for this would require additional blood and CSF collections, weeks or

398 months after the end of treatment, to determine if increased GFAP and IL-6 were transient or
399 sustained responses to senolytic treatment. Our preclinical trial of D+Q reported 35% fewer
400 insoluble NFTs in the treatment arm relative to placebo⁶, which may have reflected a reduction
401 in tangle formation and/or an increase in tau clearance. In our study, we did not observe
402 changes in total tau, p-tau-181, or p-tau-231, however, the study was not powered to assess
403 these outcomes. On-going efforts by our team are focused on a more comprehensive analyses
404 of phospho-tau in CSF and post-mortem human brain to identify which tau species best reflect
405 senescence. The results from the Lumipulse assay, but not from the SIMOA assay showed a
406 trend towards increased post-treatment A β 42 levels. If replicated in well-powered studies
407 designed to assess efficacy, the findings could suggest the possibility of disease modification
408 with senolytic treatment.

409 While our study provides the first report of senolytic treatment in humans with AD, there
410 are several important limitations that must be considered. First, our study was designed to
411 evaluate the CNS penetrance of D and Q. Therefore, it was not powered to assess outcomes
412 related to target engagement, cognition, or disease modification. The short trial duration and
413 lack of a placebo group place further restrictions on interpreting these outcomes. Another
414 limitation is the lack of established senescence and SASP markers related to AD. Prior studies
415 have reported that biomarkers of cellular senescence vary significantly across cell types and
416 inducers^{58,59}. Therefore, further work is necessary to identify clinically meaningful markers of
417 cellular senescence in AD across specimen types, and is under investigation by our team. Our
418 exploratory findings provide initial data on changes in protein levels following senolytic treatment
419 in older adults with AD, but validation and replication in well-powered randomized controlled
420 studies are critical for advancing therapeutic discovery in the field.

421 In summary, we report findings from the first clinical trial of senolytic therapy for AD. In
422 alignment with our primary study aim, we identified support for the CNS penetrance of D, although
423 Q was not detectable in CSF. In our study, the treatment was well-tolerated with excellent

424 adherence to the study drug regimen. Broader assessments of target engagement and treatment-
425 related outcomes were assessed to provide early feasibility data. While our study was not
426 designed to evaluate efficacy, the data suggests the potential of treatment-related changes in
427 markers of cellular senescence and AD pathology. Our vanguard study provides initial data on
428 the safety, tolerability, and feasibility of senolytic therapy for AD. While early results are promising,
429 fully powered, double-blinded, placebo-controlled studies are needed to evaluate the safety and
430 potential for disease modification with the novel approach of targeting cellular senescence in AD.
431

432 **Acknowledgments/Funding:** We thank the volunteers in this study and the research staff
433 who conducted recruitment and assessments. This work was made possible by grants through
434 the Alzheimer’s Drug Discovery Foundation, GC-201908-2019443 (PI: Orr), the Coordinating
435 Center for Claude D. Pepper Older Americans Independence Centers, U24AG059624; the
436 Translational Geroscience Network (R33AG061456); and the Institute for Integration of Medicine
437 & Science and the Center for Biomedical Neurosciences at UT Health Science Center in San
438 Antonio (UTHSCSA). Dr. Gonzales was supported as an RL5 Scholar in the San Antonio Claude
439 D. Pepper Older Americans Independence Center (P30AG044271) and is also supported by the
440 National Institute on Aging (R01AG077472 and P30AG066546). Dr. Garbarino is supported by
441 T32AG021890 and TR002647. Dr. Palavicini is supported by the San Antonio Claude D. Pepper
442 Older Americans Independence Center (RL5 Scholar, P30AG044271), the American Federation
443 of Aging Research, and Cure Alzheimer’s Fund. Dr. Zhang was supported by National Institute
444 on Aging (U01AG046170, R01AG068030). Dr. Musi also is supported by P30AG044271 and the
445 San Antonio Nathan Shock Center (P30AG013319). Dr. Seshadri is supported by the National
446 Institute on Aging (AG054076 and AG059421). Dr. Orr is supported by the US Department of
447 Veterans Affairs (I01BX005717), National Institute on Aging (R01AG068293, R01AG065839,
448 U54AG079754, R24AG073199), National Institute of Neurological Disorders and Stroke
449 (R21NS125171) and Cure Alzheimer’s Fund. The sponsors had no role in the design and conduct

450 of the study; in the collection, analysis, and interpretation of data; in the preparation of the
451 manuscript; or in the review or approval of the manuscript.

452 **Conflict of Interest Statement:** Dr. Gonzales reports personal stock in Abbvie. Dr. Petersen
453 reports personal fees from Roche, personal fees from Merck, personal fees from Biogen, personal
454 fees from Eisai, personal fees from Genentech, outside the submitted work. Drs. Kirkland and
455 Tchknioia have a patent Killing Senescent Cells and Treating Senescence-Associated Conditions
456 Using a SRC Inhibitor and a Flavonoid with royalties paid to Unity Biotechnologies, and a patent
457 Treating Cognitive Decline and Other Neurodegenerative Conditions by Selectively Removing
458 Senescent Cells from Neurological Tissue with royalties paid to Unity Biotechnologies. Dr. Craft
459 reports other from vTv Therapeutics, other from Cylcerion, other from T3D Therapeutics, from
460 Cognito Therapeutics, outside the submitted work. Dr. Orr has a patent Biosignature and
461 therapeutic approach for neuronal senescence pending.

462

463 **References**

- 464 1 Prince, M. J. *et al.* World Alzheimer Report 2015-The Global Impact of Dementia: An
465 analysis of prevalence, incidence, cost and trends. (2015).
- 466 2 Cummings, J., Ritter, A. & Zhong, K. Clinical trials for disease-modifying therapies in
467 Alzheimer's disease: a primer, lessons learned, and a blueprint for the future. *Journal of*
468 *Alzheimer's Disease* **64**, S3-S22 (2018).
- 469 3 Aisen, P. S. *et al.* The future of anti-amyloid trials. *The Journal of Prevention of*
470 *Alzheimer's Disease* **7**, 146-151 (2020).
- 471 4 Haass, C. & Selkoe, D. If amyloid drives Alzheimer disease, why have anti-amyloid
472 therapies not yet slowed cognitive decline? *PLoS biology* **20**, e3001694 (2022).
- 473 5 Korczyn, A. D. Mixed dementia—the most common cause of dementia. *Annals of the*
474 *New York Academy of Sciences* **977**, 129-134 (2002).
- 475 6 Musi, N. *et al.* Tau protein aggregation is associated with cellular senescence in the
476 brain. *Aging cell* **17**, e12840 (2018).
- 477 7 Dehkordi, S. K. *et al.* Profiling senescent cells in human brains reveals neurons with
478 CDKN2D/p19 and tau neuropathology. *Nature Aging* **1**, 1107-1116 (2021).
- 479 8 Kirkland, J. L. & Tchkonja, T. Cellular senescence: a translational perspective.
480 *EBioMedicine* **21**, 21-28 (2017).
- 481 9 van Deursen, J. M. The role of senescent cells in ageing. *Nature* **509**, 439-446,
482 doi:10.1038/nature13193 (2014).
- 483 10 Kritsilis, M. *et al.* Ageing, cellular senescence and neurodegenerative disease.
484 *International journal of molecular sciences* **19**, 2937 (2018).
- 485 11 Sharma, V., Gilhotra, R., Dhingra, D. & Gilhotra, N. Possible underlying influence of
486 p38MAPK and NF- κ B in the diminished anti-anxiety effect of diazepam in stressed mice.
487 *Journal of pharmacological sciences* **116**, 257-263 (2011).
- 488 12 Acosta, J. C. *et al.* A complex secretory program orchestrated by the inflammasome
489 controls paracrine senescence. *Nature cell biology* **15**, 978-990 (2013).
- 490 13 Jurk, D. *et al.* Postmitotic neurons develop a p21-dependent senescence-like phenotype
491 driven by a DNA damage response. *Aging Cell* **11**, 996-1004, doi:10.1111/j.1474-
492 9726.2012.00870.x (2012).
- 493 14 Riessland, M. *et al.* Loss of SATB1 Induces p21-Dependent Cellular Senescence in Post-
494 mitotic Dopaminergic Neurons. *Cell Stem Cell* **25**, 514-530 e518,
495 doi:10.1016/j.stem.2019.08.013 (2019).
- 496 15 Bhat, R. *et al.* Astrocyte senescence as a component of Alzheimer's disease. (2012).
- 497 16 Chinta, S. J. *et al.* Cellular Senescence Is Induced by the Environmental Neurotoxin
498 Paraquat and Contributes to Neuropathology Linked to Parkinson's Disease. *Cell Rep* **22**,
499 930-940, doi:10.1016/j.celrep.2017.12.092 (2018).
- 500 17 Streit, W. J. & Xue, Q.-S. Human CNS immune senescence and neurodegeneration.
501 *Current opinion in immunology* **29**, 93-96 (2014).
- 502 18 Bussian, T. J. *et al.* Clearance of senescent glial cells prevents tau-dependent pathology
503 and cognitive decline. *Nature* **562**, 578-582 (2018).

504 19 Zhang, P. *et al.* Senolytic therapy alleviates A β -associated oligodendrocyte progenitor
505 cell senescence and cognitive deficits in an Alzheimer's disease model. *Nature*
506 *neuroscience* **22**, 719-728 (2019).

507 20 Bryant, A. G. *et al.* Cerebrovascular senescence is associated with tau pathology in
508 Alzheimer's disease. *Frontiers in neurology* **11**, 575953 (2020).

509 21 Zhu, Y. I. *et al.* The Achilles' heel of senescent cells: from transcriptome to senolytic
510 drugs. *Aging cell* **14**, 644-658 (2015).

511 22 Lindauer, M. & Hochhaus, A. Dasatinib. *Small Molecules in Oncology*, 27-65 (2014).

512 23 Boots, A. W., Haenen, G. R. M. M. & Bast, A. Health effects of quercetin: from
513 antioxidant to nutraceutical. *European journal of pharmacology* **585**, 325-337 (2008).

514 24 Ogrodnik, M. *et al.* Cellular senescence drives age-dependent hepatic steatosis. *Nat*
515 *Commun* **8**, 15691, doi:10.1038/ncomms15691 (2017).

516 25 Tchkonja, T. & Kirkland, J. L. Aging, cell senescence, and chronic disease: emerging
517 therapeutic strategies. *Jama* **320**, 1319-1320 (2018).

518 26 Justice, J. N. *et al.* Senolytics in idiopathic pulmonary fibrosis: results from a first-in-
519 human, open-label, pilot study. *EBioMedicine* **40**, 554-563 (2019).

520 27 Hickson, L. J. *et al.* Senolytics decrease senescent cells in humans: Preliminary report
521 from a clinical trial of Dasatinib plus Quercetin in individuals with diabetic kidney
522 disease. *EBioMedicine* **47**, 446-456 (2019).

523 28 Gonzales, M. M. *et al.* Senolytic Therapy to Modulate the Progression of Alzheimer's
524 Disease (SToMP-AD): A Pilot Clinical Trial. *The Journal of Prevention of Alzheimer's*
525 *Disease* **9**, 22-29, doi:10.14283/jpad.2021.62 (2022).

526 29 Jack Jr, C. R. *et al.* Introduction to the recommendations from the National Institute on
527 Aging-Alzheimer's Association workgroups on diagnostic guidelines for Alzheimer's
528 disease. *Alzheimer's & dementia* **7**, 257-262 (2011).

529 30 Morris, J. C. Clinical dementia rating: a reliable and valid diagnostic and staging measure
530 for dementia of the Alzheimer type. *International psychogeriatrics* **9**, 173-176 (1997).

531 31 Nasreddine, Z. S. *et al.* The Montreal Cognitive Assessment, MoCA: a brief screening tool
532 for mild cognitive impairment. *Journal of the American Geriatrics Society* **53**, 695-699
533 (2005).

534 32 Corporation, P. *WMS-IV: Wechsler Memory Scale 4th Edition: Administration and*
535 *Scoring Manual*. (Harcourt, Brace, & Company, 2009).

536 33 Weintraub, S. *et al.* The Alzheimer's Disease Centers' Uniform Data Set (UDS): the
537 neuropsychologic test battery. *Alzheimer Dis Assoc Disord* **23**, 91-101,
538 doi:10.1097/WAD.0b013e318191c7dd (2009).

539 34 Tombaugh, T. N., Kozak, J. & Rees, L. Normative data stratified by age and education for
540 two measures of verbal fluency: FAS and animal naming. *Archives of clinical*
541 *neuropsychology* **14**, 167-177 (1999).

542 35 Kaplan, E., Goodglass, H. & Weintraub, S. Boston naming test. (2001).

543 36 Benedict, R. H. B., Schretlen, D., Groninger, L. & Brandt, J. Hopkins Verbal Learning Test–
544 Revised: Normative data and analysis of inter-form and test-retest reliability. *The Clinical*
545 *Neuropsychologist* **12**, 43-55 (1998).

546 37 Graf, C. The Lawton instrumental activities of daily living (IADL) scale. *The gerontologist*
547 **9**, 179-186 (2009).

548 38 Doshi, J. *et al.* MUSE: MUlti-atlas region Segmentation utilizing Ensembles of registration
549 algorithms and parameters, and locally optimal atlas selection. *Neuroimage* **127**, 186-
550 195, doi:10.1016/j.neuroimage.2015.11.073 (2016).

551 39 Srinivasan, D. *et al.* A comparison of Freesurfer and multi-atlas MUSE for brain anatomy
552 segmentation: Findings about size and age bias, and inter-scanner stability in multi-site
553 aging studies. *Neuroimage* **223**, 117248, doi:10.1016/j.neuroimage.2020.117248 (2020).

554 40 Habes, M. *et al.* The Brain Chart of Aging: Machine-learning analytics reveals links
555 between brain aging, white matter disease, amyloid burden, and cognition in the
556 iSTAGING consortium of 10,216 harmonized MR scans. *Alzheimers Dement* **17**, 89-102,
557 doi:10.1002/alz.12178 (2021).

558 41 Wilcock, D. *et al.* MarkVCID cerebral small vessel consortium: I. Enrollment, clinical, fluid
559 protocols. *Alzheimers Dement* **17**, 704-715, doi:10.1002/alz.12215 (2021).

560 42 Scalbert, A. & Williamson, G. Dietary Intake and Bioavailability of Polyphenols. *The*
561 *Journal of Nutrition* **130**, 2073S-2085S, doi:10.1093/jn/130.8.2073S (2000).

562 43 Iwashina, T. Flavonoid properties of five families newly incorporated into the order
563 Caryophyllales. *Bull Natl Mus Nat Sci* **39**, 25-51 (2013).

564 44 Porkka, K. *et al.* Dasatinib crosses the blood-brain barrier and is an efficient therapy for
565 central nervous system Philadelphia chromosome–positive leukemia. *Blood* **112**, 1005-
566 1012, doi:10.1182/blood-2008-02-140665 (2008).

567 45 Gong, X. *et al.* A Higher Dose of Dasatinib May Increase the Possibility of Crossing the
568 Blood–brain Barrier in the Treatment of Patients With Philadelphia Chromosome–
569 positive Acute Lymphoblastic Leukemia. *Clinical Therapeutics* **43**, 1265-1271.e1261,
570 doi:<https://doi.org/10.1016/j.clinthera.2021.05.009> (2021).

571 46 Erickson, M. A. & Banks, W. A. Blood–brain barrier dysfunction as a cause and
572 consequence of Alzheimer's disease. *Journal of Cerebral Blood Flow & Metabolism* **33**,
573 1500-1513 (2013).

574 47 O'Hare, T. *et al.* In vitro activity of Bcr-Abl inhibitors AMN107 and BMS-354825 against
575 clinically relevant imatinib-resistant Abl kinase domain mutants. *Cancer research* **65**,
576 4500-4505 (2005).

577 48 Sun, S. W. *et al.* Quercetin attenuates spontaneous behavior and spatial memory
578 impairment in d-galactose–treated mice by increasing brain antioxidant capacity.
579 *Nutrition Research* **27**, 169-175 (2007).

580 49 Ishisaka, A. *et al.* Accumulation of orally administered quercetin in brain tissue and its
581 antioxidative effects in rats. *Free Radical Biology and Medicine* **51**, 1329-1336,
582 doi:<https://doi.org/10.1016/j.freeradbiomed.2011.06.017> (2011).

583 50 Ren, S. C. *et al.* [Quercetin permeability across blood-brain barrier and its effect on the
584 viability of U251 cells]. *Sichuan Da Xue Xue Bao Yi Xue Ban* **41**, 751-754, 759 (2010).

585 51 Wróbel-Biedrawa, D., Grabowska, K., Galanty, A., Sobolewska, D. & Podolak, I. A
586 Flavonoid on the Brain: Quercetin as a Potential Therapeutic Agent in Central Nervous
587 System Disorders. *Life* **12** (2022).

588 52 Lundholm, M. D. & Charnogursky, G. A. Dasatinib-induced hypoglycemia in a patient
589 with acute lymphoblastic leukemia. *Clinical Case Reports* **8**, 1238-1240,
590 doi:<https://doi.org/10.1002/ccr3.2901> (2020).

- 591 53 Yu, L., Liu, J., Huang, X. & Jiang, Q. Adverse effects of dasatinib on glucose-lipid
592 metabolism in patients with chronic myeloid leukaemia in the chronic phase. *Scientific*
593 *Reports* **9**, 17601, doi:10.1038/s41598-019-54033-0 (2019).
- 594 54 Banyer, J. L., Hamilton, N. H., Ramshaw, I. A. & Ramsay, A. J. Cytokines in innate and
595 adaptive immunity. *Reviews in immunogenetics* **2**, 359-373 (2000).
- 596 55 Ito, K. *et al.* Understanding placebo responses in Alzheimer's disease clinical trials from
597 the literature meta-data and CAMD database. *Journal of Alzheimer's Disease* **37**, 173-
598 183 (2013).
- 599 56 Lamers, K. J. B. *et al.* Protein S-100B, neuron-specific enolase (NSE), myelin basic protein
600 (MBP) and glial fibrillary acidic protein (GFAP) in cerebrospinal fluid (CSF) and blood of
601 neurological patients. *Brain Research Bulletin* **61**, 261-264,
602 doi:[https://doi.org/10.1016/S0361-9230\(03\)00089-3](https://doi.org/10.1016/S0361-9230(03)00089-3) (2003).
- 603 57 Benedet, A. L. *et al.* Differences Between Plasma and Cerebrospinal Fluid Glial Fibrillary
604 Acidic Protein Levels Across the Alzheimer Disease Continuum. *JAMA Neurology* **78**,
605 1471-1483, doi:10.1001/jamaneurol.2021.3671 (2021).
- 606 58 Tuttle, C. S. L. *et al.* Cellular senescence and chronological age in various human tissues:
607 A systematic review and meta-analysis. *Aging Cell* **19**, e13083,
608 doi:<https://doi.org/10.1111/accel.13083> (2020).
- 609 59 Wiley, C. D. *et al.* Analysis of individual cells identifies cell-to-cell variability following
610 induction of cellular senescence. *Aging Cell* **16**, 1043-1050,
611 doi:<https://doi.org/10.1111/accel.12632> (2017).

612

613

614

615

616

617 Table 1: Baseline and Post-Treatment Cognitive and Functional Status Assessments

Cognitive Test	Baseline Mean (SD)	Post-Treatment Mean (SD)	T-test(df), p-value
MoCA	16.2 (2.9)	16.0 (1.1)	t(4)=-0.196, p=0.85
CDR Sum of Boxes	5.30 (2.2)	5.60 (2.0)	t(4)=2.449, p=0.070
HVLT-R Immediate Total Recall	13.80 (4.4)	10.20 (4.6)	t(4)=-3.674, p=0.021*
HVLT-R Delayed Recall	0.60 (0.9)	0.40 (0.9)	t(4)=-1.000, p=0.37
WMS Logical Memory Immediate Recall	12.6 (6.5)	13.2 (1.9)	t(4)=0.220, p=0.84
WMS Logical Memory Delayed Recall	14.2 (2.2)	12.0 (2.8)	t(4)=-1.633, p=0.18
Benson Figure Copy	8.60 (6.2)	14.6 (2.5)	t(4)=2.390, p=0.075
Benson Figure Delayed Recall	0.80 (1.5)	2.50 (3.1)	t(4)=2.049, p=0.13
Number Span Forward	6.40 (1.8)	6.80 (1.6)	t(4)=0.784, p=0.48
Number Span Backward	4.60 (1.7)	4.80 (1.3)	t(4)=0.343, p=0.75
Trails A, Time to Completion (Seconds)	76.0 (35)	99.0 (71)	t(4)=1.137, p=0.32

Trails B, Time to Completion (Seconds)	208 (86)	212 (84)	t(4)=0.829, p=0.45
Phonemic Fluency (F,A,S)	32.0 (5.8)	31.4 (5.5)	t(4)=-0.187, p=0.86
Semantic Fluency (Animals)	9.80 (1.3)	11.0 (3.2)	t(4)=1.124, p=0.32
Lawton IADL	11.0 (4.9)	10.4 (5.3)	t(4)=-0.612, p=0.57
GDS-15	4.00 (3.1)	3.60 (2.4)	t(4)=-0.459, p=0.67
NPI	5.40 (7.7)	3.80 (4.8)	t(4)=-0.758, p=0.49

618 Note: Baseline to post-treatment changes were assessed using paired samples t-tests. MoCA =

619 Montreal Cognitive Assessment, CDR = Clinical Dementia Rating scale, HVLT-R = Hopkins

620 Verbal Learning Test Revised, WMS = Weschler Memory Scales, Trails = Trail Making Test,

621 IADL = Independent Activities of Daily Living, ADL = Activities of Daily Living, GDS-15 =

622 Geriatric Depression Scale 15-Item, NPI = Neuropsychiatric Inventory, *p<0.05

623

624

625 Table 2: Baseline and Post-Treatment Neuroimaging Outcomes

Brain Region (voxels)	Baseline Mean (SD)	Post-Treatment Mean (SD)	T-test(df), p-value
Intracerebroventricular Volume (ICV)	1393962.33 (151287.55)	1393461.27 (149379.55)	t(3)=0.150, p=0.89
Total Brain Volume/ICV	0.856 (0.005)	0.851 (0.009)	t(3)=1.732, p=0.18
Grey Matter Volume/ICV	0.359 (0.021)	0.359 (0.015)	t(3)=0.522, p=0.64
White Matter Volume/ICV	0.452 (0.006)	0.446 (0.009)	t(3)=1.192, p=0.32
Right Hippocampus Volume/ICV	0.002 (0.00016)	0.0002 (0.00013)	t(3)=0.472, p=0.67
Left Hippocampus Volume/ICV	0.002 (0.00008)	0.002 (0.00012)	t(3)=0.313, p=0.77

626

627 Note: Baseline to post-treatment changes were assessed using paired samples t-tests. Brain
628 regions normalized to intracerebroventricular volume (ICV) measured in voxels, p<0.05.

629

630

631 Table 3: Significantly Differentially Expressed Proteins in Plasma and Cerebrospinal Fluid from
 632 Baseline to Post-Treatment

Protein (pg/mL)	Baseline Mean (SD)	Post-Treatment Mean (SD)	Fold Change	T-test(df), p-value
Plasma				
*IL6	1.30 (0.54)	1.58 (0.81)	1.22	t(4)= 1.651, p=0.145
IL-17E	25.2 (20.3)	17.0 (14.5)	0.67	t(4)= -5.216, p=0.0014
IL-21	166 (96.7)	102 (72.1)	0.62	t(4)=-4.714, p=0.002
IL-23	53.4 (29.5)	34.0 (25.4)	0.64	t(4)=-4.345, p=0.003
IL-17A/F	35.4 (12.8)	23.1 (12.7)	0.65	t(4)=-3.870, p=0.007
IL-17D	67.7 (25.5)	49.0 (17.9)	0.72	t(4)=-3.384, p=0.013
IL-10	0.31 (1.0)	0.21 (0.20)	0.66	t(4)=-3.347, p=0.013
VEGF	20.8 (6.0)	12.5 (3.4)	0.60	t(4)=-3.238, p=0.015
YKL-40	58047 (60143)	105444 (127256)	1.82	t(4)=3.017, p=0.020
IL-31	67.5 (27.9)	54.8 (28.9)	0.81	t(4)=-2.914, p=0.024
MCP-2	23.5 (5.1)	18.5 (4.5)	0.79	t(4)=-2.806, p=0.028
MIP-1 β	48.5 (16.1)	36.9 (25.8)	0.76	t(4)=-2.515, p=0.042
MIP-1 α	24.3 (1.6)	19.6 (4.7)	0.81	t(4)=-2.433, p=0.047
Cerebrospinal Fluid				
*IL-6	1.16 (0.32)	1.55 (0.23)	1.34	t(4)=3.913, p=0.008
TARC	1.42 (0.42)	1.25 (0.38)	0.87	t(4)=-3.099, p=0.021
IL-17A	0.54 (0.13)	0.35 (0.11)	0.60	t(4)=-2.753, p=0.033
I-TAC	4.15 (1.2)	3.36 (1.1)	0.81	t(4)=-2.736, p=0.033
Eotaxin-2	14.5 (6.5)	12.8 (5.3)	0.89	t(4)=-2.630, p=0.038
Eotaxin	16.9 (4.9)	14.7 (4.3)	0.87	t(4)=-2.534, p=0.044

MIP-1 α	19.0 (2.4)	14.3 (4.8)	0.75	t(4)=-2.471, p= 0.048
<p>Note: Differential expression analysis was carried out by the moderated t-test *: Prespecified secondary outcome IL = interleukin, MIP = Macrophage Inflammatory Protein, G-CSF = Granulocyte Colony-Stimulating Factor, TRAIL = Tumor Necrosis Factor Related Apoptosis-Inducing Ligand, TARC = Thymus- and Activation-Regulated Chemokine, p<0.05</p>				

634 Supplementary Table 1: Baseline and Post-Treatment Safety Labs

Blood Marker	Baseline Mean (SD)	Post- Treatment Mean (SD)	T-test(df), p-value
White blood cells (K/uL)	7.0 (2.3)	5.8 (1.8)	t(4)=-1.197, p=0.30
Red blood cells (MIL/uL)	4.5 (0.7)	4.5 (0.8)	t(4)=-0.726, p=0.51
Hemoglobin (g/dl)	14.0 (1.7)	14.0 (1.8)	t(4)=-0.215, p=0.84
Hematocrit (%)	41.8 (5.)	41.1 (6.6)	t(4)=-0.497, p=0.65
MCV (fL)	92.2 (2.7)	92.6 (2.7)	t(4)=0.667, p=0.54
MCH (pg)	31.0 (1.3)	31.6 (1.8)	t(4)=1.199, p=0.30
MCHC (g/dl)	33.6 (1.8)	34.2 (1.4)	t(4)=0.756, p=0.49
RDW (%)	12.6 (0.6)	12.6 (0.5)	t(4)=-0.279, p=0.79
Platelets (K/uL)	224.0 (69.5)	235.8 (77.8)	t(4)=0.717, p=0.51
Absolute Neutrophils (K/uL)	69.0 (6.6)	64.4 (2.2)	t(4)=-1.696, p=0.17
Absolute Lymphocyte (K/uL)	19.0 (6.2)	22.2 (4.8)	t(4)=1.536, p=0.20
Absolute Monocyte (K/uL)	8.8 (1.9)	9.8 (2.8)	t(4)=1.826, p=0.14

Absolute Eosinophil (K/uL)	2.2 (0.8)	2.2 (0.5)	t(4)<0.001, p=1.0
Absolute Basophil (K/uL)	0.8 (0.5)	1.0 (0)	t(4)=1.000, p=0.37
Glucose (mg/dL)	91.4 (14.6)	87.6 (24.2)	t(4)=-0.656, p=0.55
Blood Urea Nitrogen (mg/dL)	17.6 (6.5)	16.0 (1.7)	t(4)=-0.726, p=0.51
Creatinine (mg/dL)	0.90 (0.15)	0.86 (0.15)	t(4)=-0.539, p=0.62
eGFR (mL/min/1.73)	73.2 (10.6)	79.6 (9.6)	t(4)=1.082, p=0.34
Sodium (mmol/L)	140.4 (1.5)	141.0 (2.1)	t(4)=0.440, p=0.68
Potassium (mmol/L)	4.3 (0.3)	4.2 (0.3)	t(4)=-0.250, p=0.81
Calcium (mg/dL)	9.5 (0.5)	9.4 (0.5)	t(4)=-1.725, p=0.16
Total Protein (g/dL)	6.7 (0.5)	6.6 (0.4)	t(4)=-2.359, p=0.078
Albumin (g/dL)	4.3 (0.2)	4.2 (0.2)	t(4)=-1.000, p=0.37
Bilirubin (mg/dL)	0.6 (0.3)	0.4 (0.1)	t(4)=-2.236, p=0.089
Alkaline Phosphate (IU/L)	73.2 (23.7)	75.2 (23.7)	t(4)=0.381, p=0.72
Aspartate Aminotransferase (IU/L)	21.2 (6.2)	21.6 (4.2)	t(4)=0.209, p=0.84
Alanine Transaminase (IU/L)	15.6 (3.6)	17.0 (5.2)	t(4)=0.560, p=0.61
Total Cholesterol (mg/dL)	169.2 (35.5)	179.4 (40.0)	t(4)=2.904, p=0.044*
Triglycerides, (mg/dL)	79.6 (9.4)	102.0 (13.5)	t(4)=2.535, p=0.064

HDL-Cholesterol (mg/dL)	68.6 (20.0)	67.6 (21.7)	t(4)=-0.632, p=0.56
LDL-Cholesterol (mg/dL)	85.5 (17.9)	93.8 (21.9)	t(4)=2.493, p=0.067
Hemoglobin A1c (%)	5.4 (0.4)	5.3 (0.2)	t(4)=-0.739, p=0.50

635 *p<0.05

636 **Figure Legends**

637 Figure 1: Study Design and Timeline. Modified from Gonzales et al., 2021²⁸. Primary outcomes
638 were to assess blood-brain barrier penetrance of the senolytic drugs Dasatinib (D) and
639 Quercetin (Q) (D+Q). Secondary outcomes explored target engagement, safety, functional
640 outcomes and neuroimaging markers.

641 Figure 2: CONSORT Flow Diagram. Participant allocation in the open-label pilot study.

642 Figure 3: Concentration of D (Post-Treatment) and Q (Pre- and Post-Treatment) concentrations
643 in blood and CSF quantified by High Performance Liquid Chromatography (HPLC) with Tandem
644 Mass Spectrometry detection (MS/MS) method (HPLC/MS/MS).

645 Figure 4: Baseline and Post-Treatment Alzheimer's Disease and Related Dementia Plasma and
646 Cerebrospinal Fluid Biomarkers Assessed Using the Simoa HD-X Analyzer. Values derived
647 from paired samples t-test and p-value of 0.05.

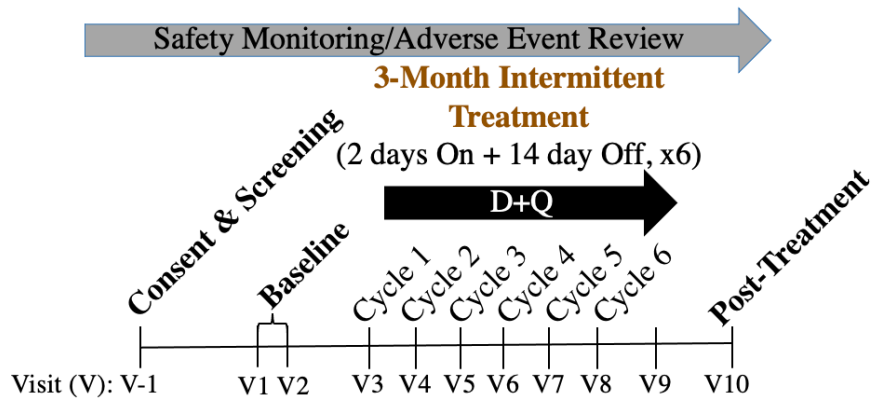
648 Figure 5: Baseline and Post-Treatment Alzheimer's Disease and Related Dementia
649 Cerebrospinal Fluid Biomarkers Assessed Using the Lumipulse. Values derived from paired
650 samples t-test and p-value of 0.05

651

652

653

654



Primary Outcomes:

Blood Brain Barrier Penetrance

Secondary Outcomes:

Target Engagement

Safety

Cognitive/Functional/Physical

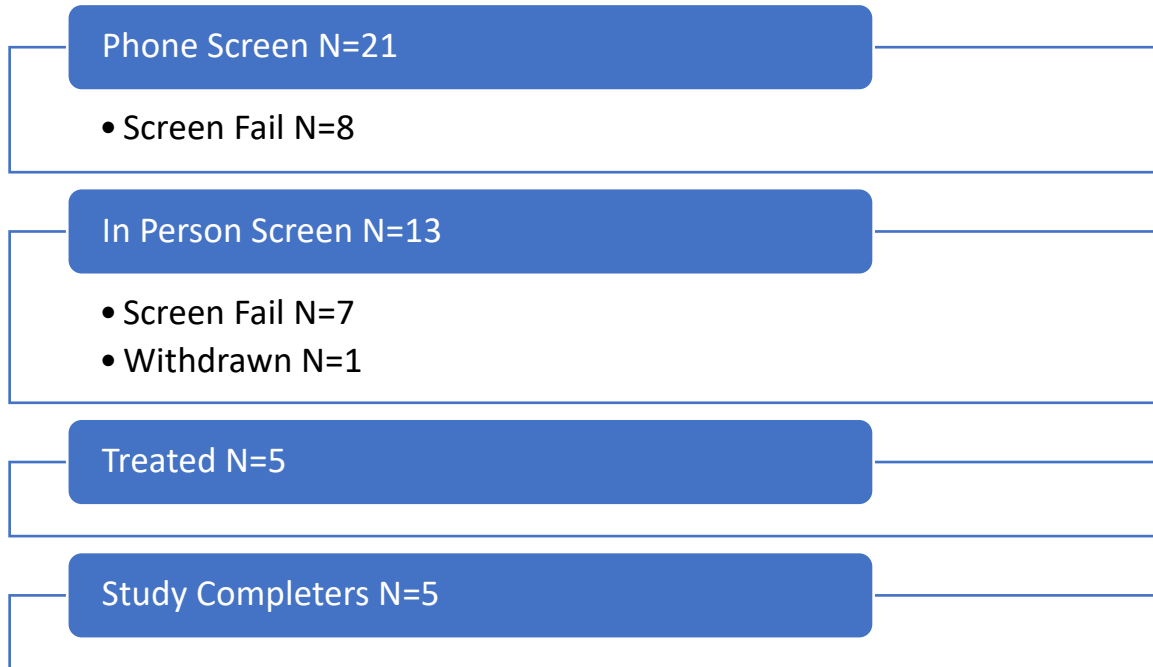
Neuroimaging Markers

Blood Brain Barrier Penetrance		✓								✓
Target Engagement		✓								✓
Safety	✓	✓	✓	✓	✓	✓	✓	✓	✓	✓
Cognitive/Functional/Physical		✓								✓
Neuroimaging Markers		✓								✓

655

656 **Figure 1:** Study Design and Timeline

657



658

659 **Figure 2.** CONSORT Flow Diagram

660

661

662

663

664

665

666

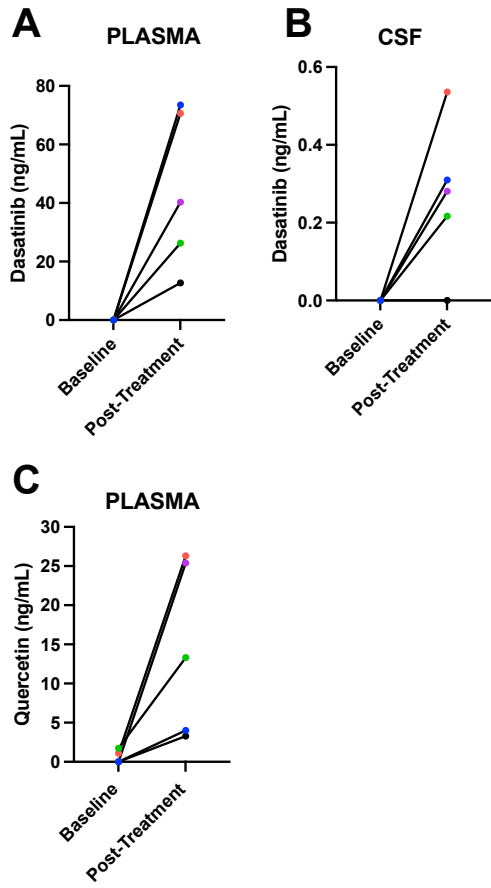
667

668

669

670

671



672

673 **Figure 3.** D+Q Plasma and CSF Concentrations

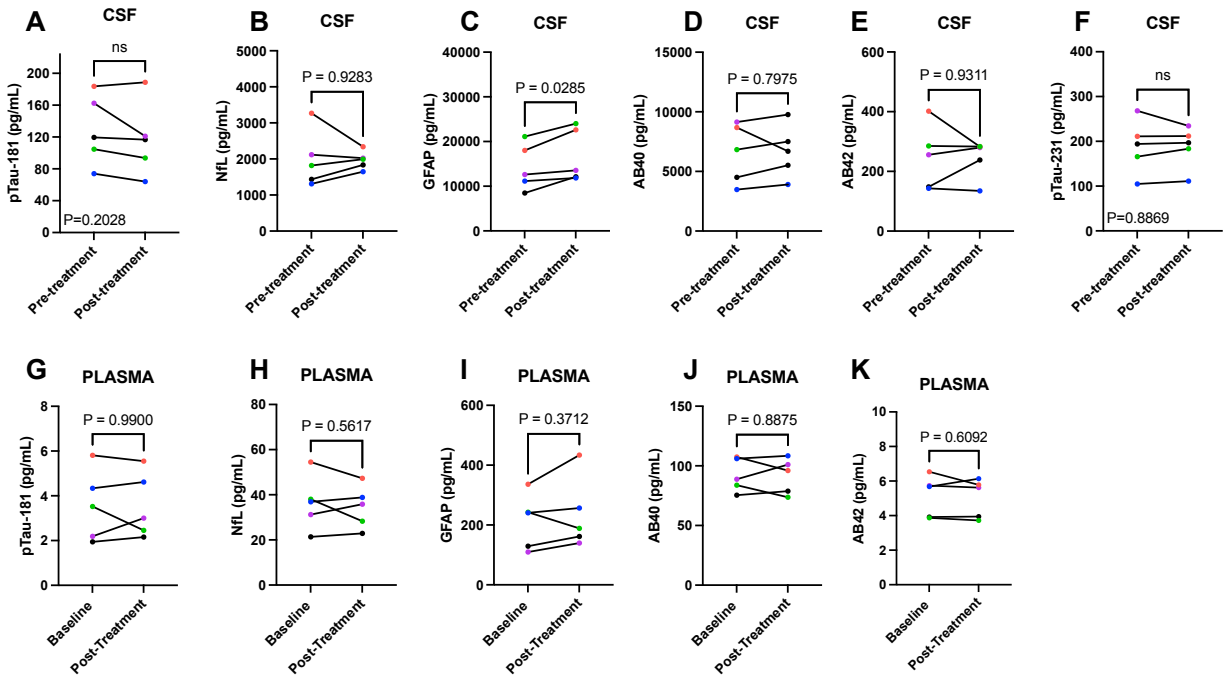
674

675

676
677

678

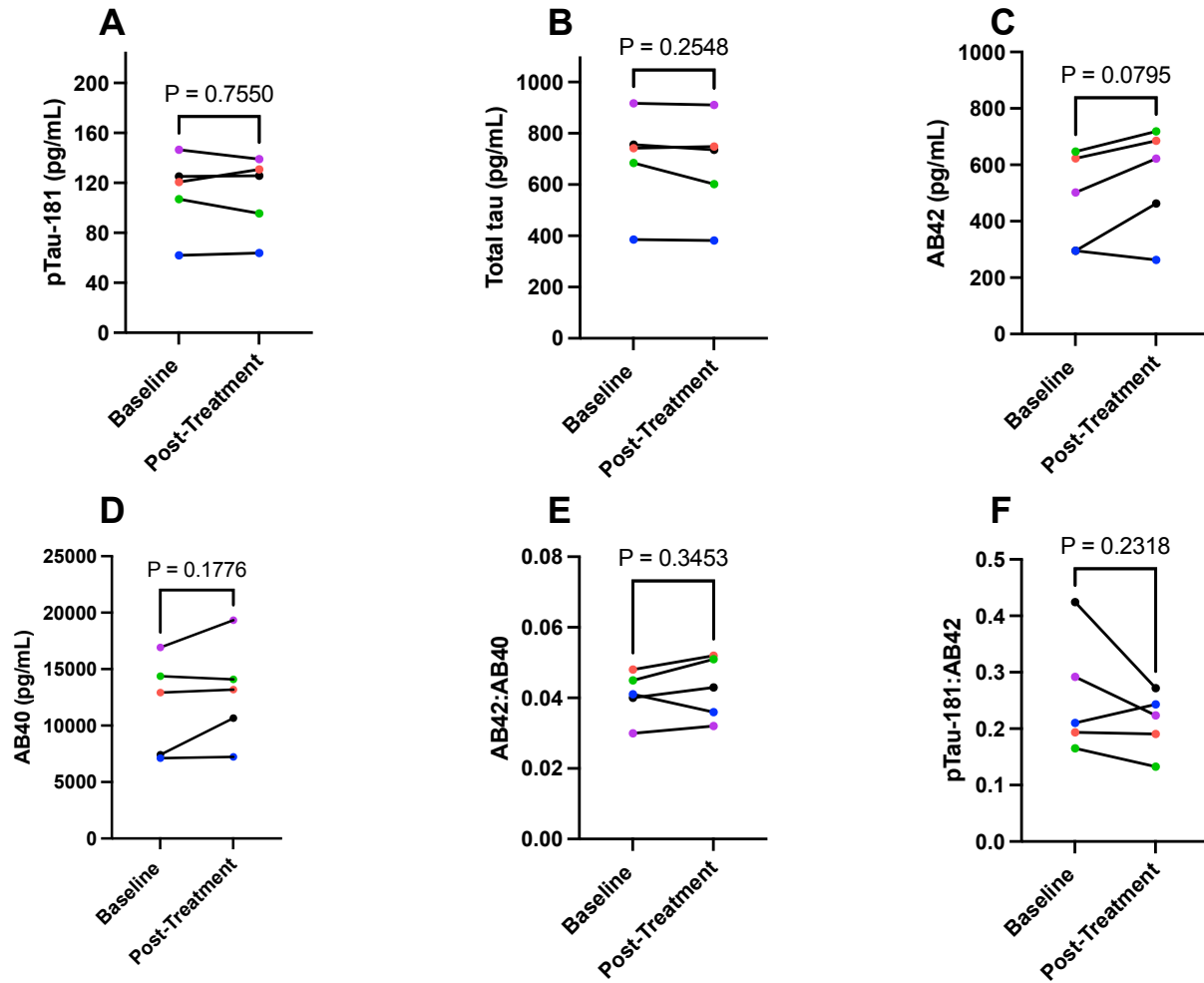
679



680

681 **Figure 4.** Baseline and Post-Treatment Alzheimer's Disease and Related Dementia Plasma and

682 Cerebrospinal Fluid Biomarkers



683

684 **Figure 5.** Baseline and Post-Treatment Alzheimer's Disease and Related Dementia

685 Cerebrospinal Fluid Biomarkers

686